Slow round-trip variations across quantum and classical critical points

Francesco Tarantelli
francesco.tarantelli@phd.unipi.it

Tarantelli, Vicari PR B 105 235124 (2022)

University of Pisa and INFN

19^{th} December

Introduction

- We address out-of-equilibrium dynamics of many-body systems subject to round-trip protocols across quantum and classical phase transitions;

- We perform Kibble-Zurek(KZ) protocols which develop dynamic scaling behavior at both the transitions obtained from a Renormalization Group(RG) framework;

- While classical and quantum models, belonging to the same universality class, show similar dynamic scaling frameworks, substantial differences emerge in the round-trip evolution.

Classical Ising Model

2D Classical Ising Hamiltonian with size LxL and with PBC:

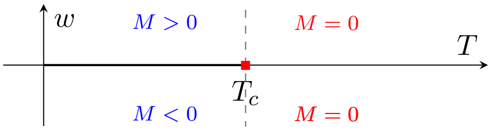

$$H_{\rm cl} = -J \sum_{\langle i,\, j\rangle} S_i \cdot S_j - w \cdot \sum_i S_i \ , \qquad (1)$$

$$Z = \sum_{\{S_i\}} e^{-H/T} \ ; \qquad (2)$$

Continuous Transition point: at $w = 0$ and $T_c = \frac{2}{\ln(1+\sqrt{2})}$ $(J = 1 \text{ fixed})$

RG dimensions:

$$w \longrightarrow y_w = 15/8 \qquad T \longrightarrow y_t = 1 \qquad \text{Metropolis time } t \longrightarrow z = 2.1667(5) \ .$$

Quantum Ising Model

1D Quantum Ising Hamiltonian for a chain of size L and PBC ($\hat{\sigma}^{(k)}_{L+1} = \hat{\sigma}^{(k)}_{1}$):

$$\hat{H}_{\text{Is}} = -\sum_{x=1}^{L} \hat{\sigma}^{(1)}_x \hat{\sigma}^{(1)}_{x+1} - g\sum_{x=1}^{L} \hat{\sigma}^{(3)}_x - w\sum_{x=1}^{L} \hat{\sigma}^{(1)}_x \; ; \tag{3}$$

$\sigma^{(k)}_x$ are the Pauli matrices on the x^{th} site in the k-axis direction.

Continuous Transition point: at $w = 0$ and $g_c = 1$

RG dimensions:

$$w \longrightarrow y_w = 15/8 \quad r = g - g_c \longrightarrow y_r = 1 \quad \text{time } t \longrightarrow z = 1 \tag{4}$$
$$\hat{\sigma}^{(1)}_x \longrightarrow y_l = d + z - y_h = 1/8 \; .$$

Kitaev Model

Kitaev Hamiltonian mapped into a spin-$1/2$ XY chain, by a Jordan-Wigner transformation (OBC): $\hat{c} \longrightarrow \hat{\sigma}$

$$\hat{H}_K^{(\mathrm{ABC})} = -\sum_{x=1}^{L}\Big[\big(\hat{c}_x^\dagger\,\hat{c}_{x+1} + \hat{c}_{x+1}^\dagger\,\hat{c}_x\big) + \delta\,\big(\hat{c}_x\,\hat{c}_{x+1} + \hat{c}_{x+1}^\dagger\,\hat{c}_x^\dagger\big)\Big] - \sum_{x=1}^{L}\mu\,\hat{c}_x^\dagger\,\hat{c}_x\ ; \quad (5)$$

Continuous Transition point:

$$\mu_c = -2 \qquad \text{and} \qquad \delta = 1 \text{ fixed}\ ;$$

RG dimensions:

$$w = \mu - \mu_c \longrightarrow y_w = 1 \qquad \hat{c}_x\,,\ \hat{c}_x^\dagger \longrightarrow y_c = 1/2 \qquad \text{dynamic exp}: z = 1\ .$$

Kibble Zurek(KZ) Protocol

(i) Start at the equilibrium state (classical) and at the ground state $|\Psi(t = t_i)\rangle \equiv |\Psi(w_i < 0)\rangle$ (quantum);

(ii) quantum case:

$$\frac{d\,|\Psi(t)\rangle}{dt} = -i\hat{H}[w(t)]\,|\Psi(t)\rangle \;\; ;$$

(ii) classical one:

Metropolis algorithm;

$$\Downarrow$$

$$w(t) = t/t_s \;\; ;$$

from $w_i < 0$ to $w_f > 0$, where t_s is the time scale of the slow variations of w.

(iii) Then, for $t > t_f$, $w(t)$ decreases with the same t_s, from $w_f > 0$ to the original value $wi < 0$, closing the cycle.

F.T., E.V. PR B 105 235124

Observables

Classical Ising model

$$M(t) = \frac{1}{L^2}\sum_i \langle S_i \rangle_t \quad ; \tag{6}$$

$$G(t, \boldsymbol{x}, \boldsymbol{y}) \equiv \langle s_{\boldsymbol{x}}\, s_{\boldsymbol{y}} \rangle_t \, . \tag{7}$$

Quantum models

Adiabaticity function:

$$A(t) = \Big| \langle \Psi_0[w(t)] | \Psi(t) \rangle \Big| \, ; \tag{8}$$

Ising:

$$M(t) \equiv \frac{1}{L}\sum_x \langle \Psi(t)|\, \sigma_x^{(1)} |\Psi(t)\rangle \, ;$$

Kitaev:

$$C(x,t) \equiv \langle \Psi(t)|\, c_j^\dagger c_{j+x} + c_{j+x}^\dagger c_j \,|\Psi(t)\rangle \, .$$

Dynamic scaling framework for the round-trip

The asymptotic dynamic FSS behavior is obtained by taking $t_s \to \infty$ and $L \to \infty$:

$$\begin{aligned} K &= w(t) L^{y_w}\,, & \Upsilon &= t_s / L^{\zeta}\,, \\ \Theta_i &= w_i\, t_s^{1-\kappa}\,, & \Theta &= w(t)\, t_s^{1-\kappa} = t / t_s^{\kappa}\,, \end{aligned} \tag{9}$$

where

$$\zeta = y_w + z\,, \qquad \kappa = z/\zeta\,, \qquad 1 - \kappa = y_w / \zeta\,. \tag{10}$$

with $w_f = -w_i = w_\star$, we have:

$$\Upsilon = t_s / L^{\zeta}\,, \quad \Theta = w(t)\, t_s^{1-\kappa}\,, \quad \Theta_\star = w_\star\, t_s^{1-\kappa}\,. \tag{11}$$

Numerical results - Classical Ising

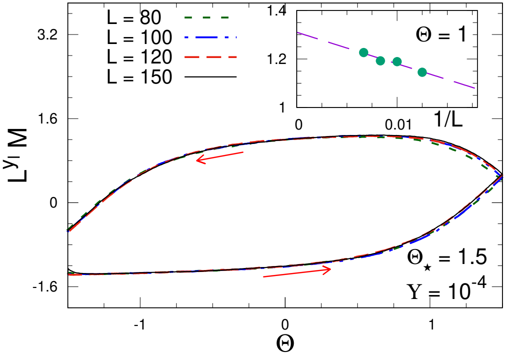

Figure 1:
$M^{(a/b)}(t,t_s,w_\star,L) \approx L^{-y_l}\mathcal{M}_i(\Upsilon,\Theta,\Theta_\star)$
$\Upsilon = 10^{-4}$, fixed $\Theta_\star = 1.5$ and plotted versus $\Theta = w(t)t_s^{1-\kappa}$.

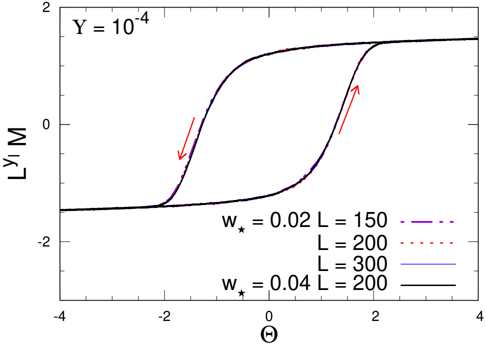

Figure 2: Thermalized classical state for fixed $\Upsilon = 10^{-4}$, and fixed $w_\star = 0.02$ and $w_\star = 0.04$.

Numerical results - Quantum Ising

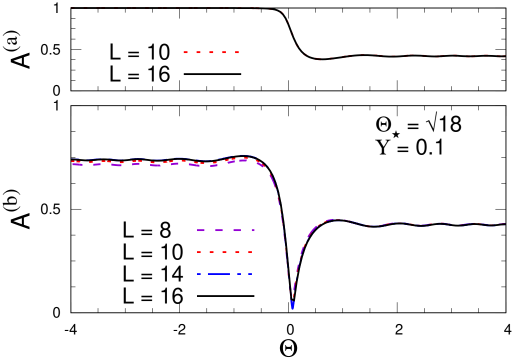

Figure 3: $A^{(a/b)}(t, t_s, w_\star, L) \approx \mathcal{A}^{(a/b)}(\Upsilon, \Theta, \Theta_\star)$; fixed $\Upsilon = t_s/L^\zeta = 0.1$ and $\Theta_\star = w_\star L^{1-\kappa} = \sqrt{18}$, for the outward (top) and return (bottom).

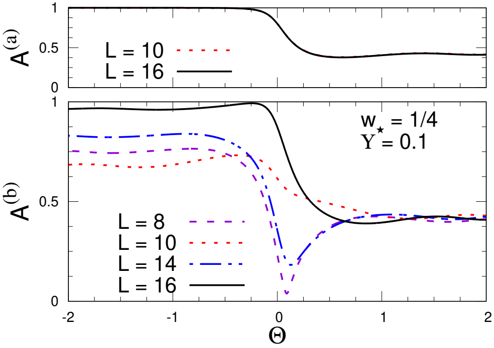

Figure 4: Fixed $\Upsilon = 0.1$ and $w_\star = 1/4$, for the outward (top) and return (bottom), versus $\Theta = w(t)L^{1-\kappa}$.

Numerical results - Kitaev chain

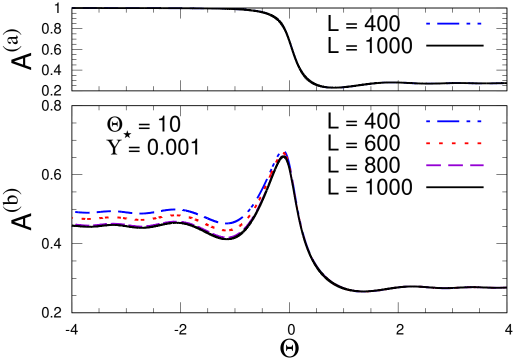

Figure 5: $A^{(a/b)}(t, t_s, w_\star, L) \approx \mathcal{A}^{(a/b)}(\Upsilon, \Theta, \Theta_\star)$; Finite $\Theta_\star = 10$ at fixed $\Upsilon = t_s/L^\zeta = 0.001$ and $\Theta_\star = w_\star L^{1-\kappa} = 10$, for outward and return.

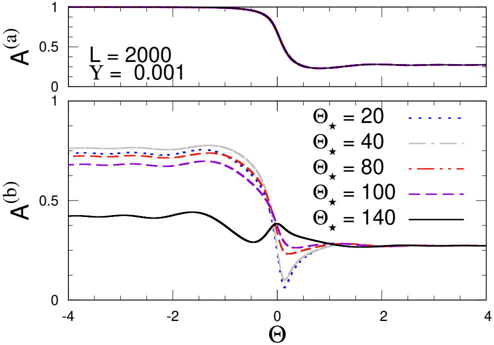

Figure 6: At $L = 2000$ and $\Upsilon = 0.001$ for the outward (top) and return (bottom), versus Θ, for various $\Theta_\star$.

F.T., E.V. PR B 105 235124

The limit $\Theta_\star \to \infty$

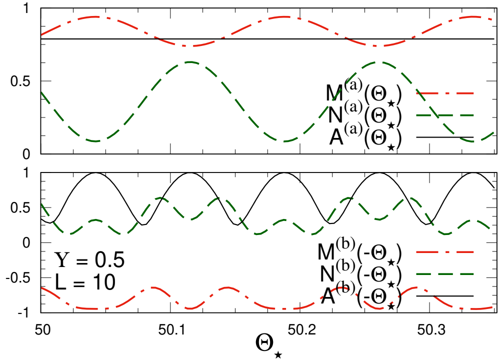

Figure 7: **Ising** - Fixed $L = 10$, $\Upsilon = 0.5$ versus $\Theta_\star$, close to $\Theta_\star = 50$. The top plot shows the values at $\Theta = \Theta_\star$, while the bottom plot the values at $\Theta = -\Theta_\star$.

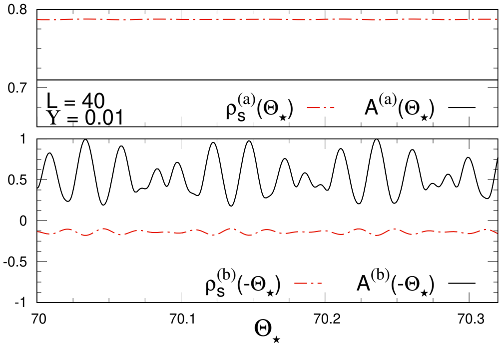

Figure 8: **Kitaev** - Fixed $L = 40$, $\Upsilon = 0.01$ versus $\Theta_\star$, close to $\Theta_\star = 70$. The top plot shows the values at $\Theta = \Theta_\star$, while the bottom at $\Theta = -\Theta_\star$.

F.T., E.V. PR B 105 235124

Two-Level Model: $H_{2\ell}(t) = -\beta(t)\sigma^{(3)} + \frac{\Delta}{2}\sigma^{(1)}$

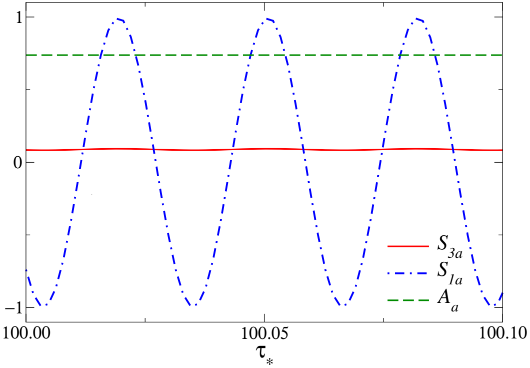

Figure 9: Dependence on $\tau_\star \equiv t_\star/\sqrt{t_s}$ at the end of the first dynamic branch for $\upsilon = 1$, and $\tau_\star \approx 100$.

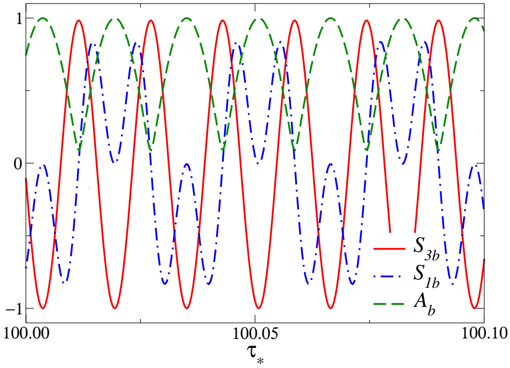

Figure 10: Dependence on $\tau_\star$ at the end of round-trip protocol for $\upsilon = t_s\Delta^2 = 1$, and $\tau_\star \approx 100$.

Conclusions

- We studied the out-of-equilibrium behavior when Hamiltonian parameters slowly cross phase transition;
- We extend the RG framework from the standard one-way KZ protocols to the round-trip one;
- Analogy of the scaling behaviors at classical and quantum transitions is only partially extended to round-trip KZ protocols. Substantial differences emerge:
  1. classical systems develop scaling hysteresis-like scenarios,
  2. in quantum systems, the persistence of oscillating relative phases make the return way extremely sensitive to the parameters of the protocol;
- Even in the simple two-level quantum model, we have a similar behavior.